Quaternary Science Reviews 30 (2011) 3234–3247

Contents lists available at ScienceDirect

Quaternary Science Reviews

journal homepage: www.elsevier.com/locate/quascirev

Ocean circulation, ice sheet growth and interhemispheric coupling of millennial climate variability during the mid-Pleistocene (ca 800–400 ka)

M. Alonso-Garcia [a,*], F.J. Sierro [a], M. Kucera [b], J.A. Flores [a], I. Cacho [c], N. Andersen [d]

[a] Department of Geology (Paleontology), Faculty of Science, University of Salamanca, Pza. de la Merced s/n, 37188 Salamanca, Spain
[b] Institute of Geosciences (Micropaleontology), University of Tübingen, Sigwartstrasse 10, DE-72076 Tübingen, Germany
[c] Department of Stratigraphy, Paleontology and Marine Geosciences, Faculty of Geology, University of Barcelona, Martí i Franquès s/n, 08028 Barcelona, Spain
[d] Leibniz Laboratory for Radiometric Dating and Stable Isotope Research, University of Kiel, Max-Eyth-Str. 11, 24118 Kiel, Germany

ARTICLE INFO

Article history:
Received 9 September 2010
Received in revised form
28 May 2011
Accepted 5 August 2011
Available online 25 September 2011

Keywords:
North Atlantic
Mid-Pleistocene
Stable isotopes
Foraminifera
IRD
IODP Site U1314

ABSTRACT

Stable carbon and oxygen isotopes from benthic and planktic foraminifers, planktic foraminifer assemblages and ice rafted debris from the North Atlantic Site U1314 (Integrated Ocean Drilling Program Expedition 306) were examined to investigate orbital and millennial-scale climate variability in the North Atlantic and its impact on global circulation focusing on the development of glacial periods during the mid-Pleistocene (ca 800–400 ka). Glacial initiations were characterized by a rapid cooling (6–10 °C in less than 7 kyr) in the mean annual sea surface temperature (SST), increasing benthic $\delta^{18}O$ values and high benthic $\delta^{13}C$ values. The continuous increase in benthic $\delta^{18}O$ suggests a continuous ice sheet growth whereas the positive benthic $\delta^{13}C$ values indicate that the flow of the Iceland Scotland Overflow water (ISOW) was vigorous. Strong deep water formation in the Norwegian Greenland Sea promoted a high transfer of freshwater from the ocean to the continents. However, low SSTs at Site U1314 suggest a subpolar gyre cooling and freshening that may have reduced deep water formation in the Labrador Sea during glacial initiations.

Once the 3.5‰ threshold in the benthic $\delta^{18}O$ record was exceeded, ice rafting started and ice sheet growth was punctuated by millennial-scale waning events which returned to the ocean part of the freshwater accumulated on the continents. Ice-rafting events were associated with a rapid reduction in the ISOW (benthic $\delta^{13}C$ values dropped 0.5–1‰) and followed by millennial-scale warmings. The first two millennial-scale warm intervals of each glacial period reached interglacial temperatures and were particularly abrupt (6–10 °C in ~3 kyr). Subsequent millennial-scale warm events were cooler probably because the AMOC was rather reduced as suggested by the low benthic $\delta^{13}C$ values. These two abrupt warming events that occurred at early glacial periods were also observed in the Antarctic temperature and CO_2 records, suggesting a close correlation between both Hemispheres. The comparison of the sea surface proxies with the benthic $\delta^{18}O$ record (as the Southern sign) indicates the presence of a millennial-scale seesaw pattern similar to that seen during the Last Glacial period.

1. Introduction

One of the most outstanding features of Pleistocene climate is the succession of glacial and interglacial periods. During the Early Pleistocene climate cyclicity was driven by obliquity and glacial–interglacial cycles occurred approximately every 41 kyr (Imbrie et al., 1993). The periodicity of the climatic cycles shifted during the mid-Pleistocene from the obliquity-dominated cycles to an eccentricity-dominated cycle of ~100 kyr. While the climatic shift from the "41 kyr world" to the "100 kyr world" may be related to changes in the internal feedbacks of the climate system, the detailed mechanisms/processes are not fully understood (Imbrie et al., 1993; Berger and Jansen, 1994; Mudelsee and Stattegger, 1997; Maslin and Ridgwell, 2005). For instance, ice sheet size and the severity of glacial periods began to increase at ~910 ka but the dominance of the 100 kyr cycles only started at 650–725 ka (Mudelsee and Schulz, 1997; Mudelsee and Stattegger, 1997). Moreover, only the last four climatic cycles (last ~420 ka) exhibit strong interglacial conditions (Jansen et al., 1986; Berger and Wefer, 2003; Tzedakis et al., 2009).

Mid-Pleistocene glacial–interglacial cycles exhibit similar changes in thermohaline circulation strength as compared to the last climatic cycle with strong circulation during interglacial periods, weak during glacial periods and even weaker during the major ice-

* Corresponding author. Present address: College of Marine Science, University of South Florida, 140 7th Avenue South, St. Petersburg, FL 33701, USA. Tel.: +1 7275531002.
E-mail address: montserrat@mail.usf.edu (M. Alonso-Garcia).

0277-3791/$ – see front matter © 2011 Elsevier Ltd. All rights reserved.
doi:10.1016/j.quascirev.2011.08.005

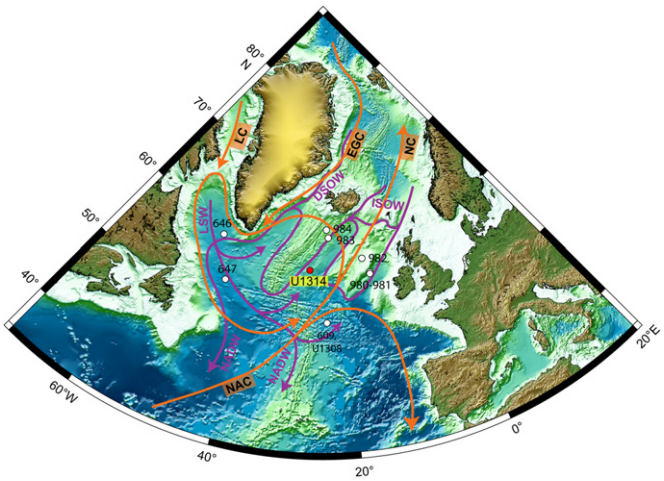

Fig. 1. Location of IODP Site U1314 (red dot) and other ODP North Atlantic sites mentioned in the paper (white dots). Orange arrows represent North Atlantic surface circulation after Schmitz and McCartney (1993). Purple arrows represent deep ocean circulation after Dickson et al. (1990). EGC: East Greenland Current; NC: Norwegian Current; LC: Labrador Current; NAC: North Atlantic Current; DSOW: Denmark Strait Overflow water; ISOW: Iceland Scotland Overflow water; LSW: Labrador Sea water; NADW: North Atlantic Deep water. The base map was provided by IODP. (For interpretation of the references to colour in this figure legend, the reader is referred to the web version of this article.)

rafting events (Raymo et al., 1990, 1997, 1998, 2004; deMenocal et al., 1992; Oppo et al., 1995, 1998; McManus et al., 1999; Venz et al., 1999; Flower et al., 2000; Venz and Hodell, 2002; Hodell et al., 2003, 2008; Kleiven et al., 2003; Hodell and Venz-Curtis, 2006). During glacial periods, North Atlantic bottom waters were characterized by very low $\delta^{13}C$ values, indicating the presence of the Southern Ocean Water (SOW), whereas $\delta^{13}C$ values at depths above ~2000 to 2200 m were significantly higher suggesting a North Atlantic origin for this shallower water mass, known as Glacial North Atlantic Intermediate water (GNAIW) (Boyle and Keigwin, 1982, 1987; Curry and Lohmann, 1983; Oppo and Fairbanks, 1987; Curry et al., 1988; Duplessy et al., 1988; Curry and Oppo, 2005; Marchitto and Broecker, 2006). North Atlantic sediments suggest that during the Last Glacial period the ice sheet growth has been punctuated by several major ice-rafting events followed by prominent warm interstadials associated with rapid global sea level rise (Heinrich, 1988; Bond et al., 1992, 1993 Broecker et al., 1992; Grousset et al., 1993; Chapman and Shackleton, 1999; Shackleton et al., 2000; Siddall et al., 2003; Hemming, 2004; Arz et al., 2007; Rohling et al., 2008; Sierro et al., 2009). Furthermore, the iceberg discharges have also been associated with strong reductions in Atlantic Meridional Overturning Circulation (AMOC). Similar ice-rafting events associated with reductions in the AMOC have been reported from mid-late Pleistocene North Atlantic sediments (Oppo et al., 1998; Raymo et al., 1998; McManus et al., 1999; Venz et al., 1999; Hodell et al., 2003, 2008). Millennial-scale climate instability has been a pervasive long-term characteristic of Earth's climate (Raymo et al., 1998; Siddall et al., 2006) and it suggests that the processes that drove millennial-scale climate changes could have

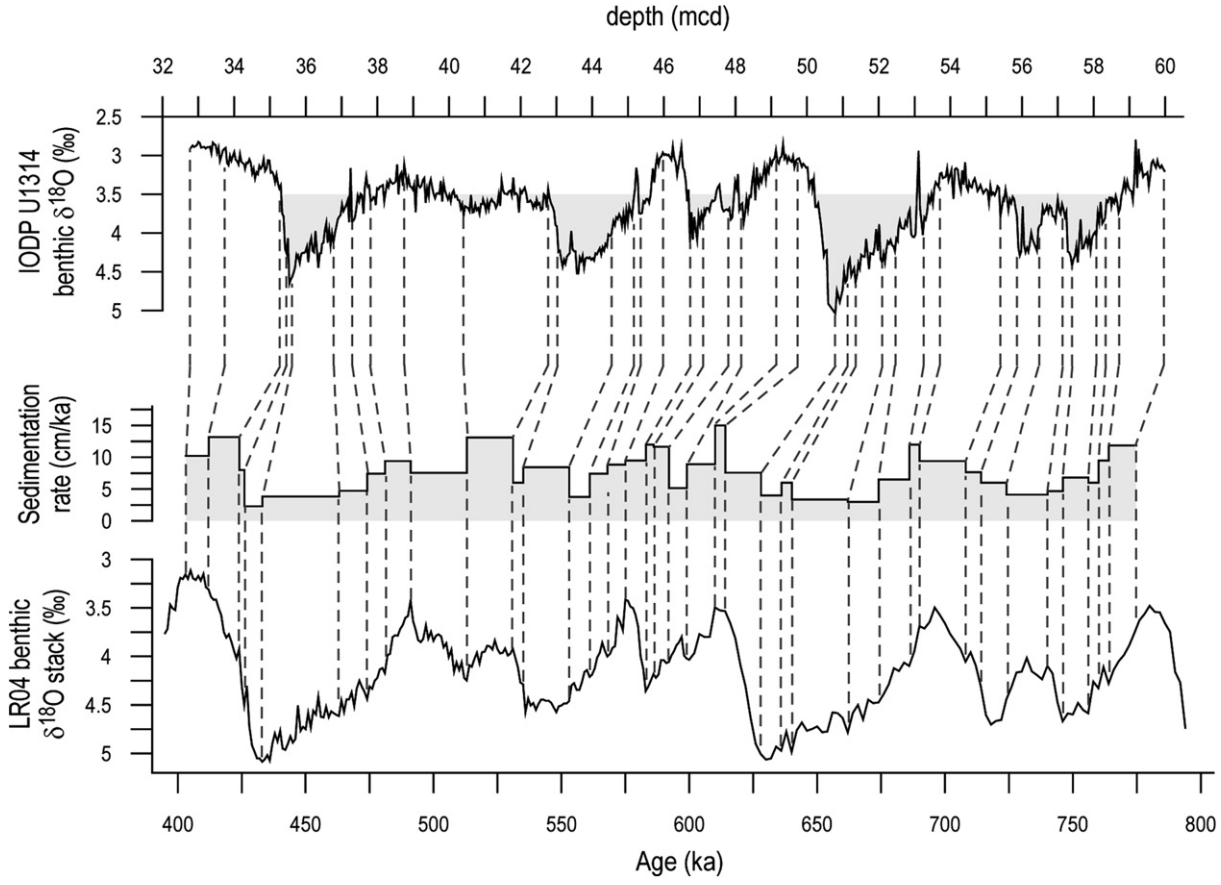

Fig. 2. The age model of the studied interval was derived by correlating the benthic $\delta^{18}O$ record of Site U1314 with the LR04 benthic $\delta^{18}O$ stack (Lisiecki and Raymo, 2005). The benthic $\delta^{18}O$ record of Site U1314 is shown in meters of composite depth (mcd) whereas the LR04 benthic $\delta^{18}O$ stack is shown in its age scale. The tie points of both records are joined with grey dashed lines and the sedimentation rates for each interval between the tie points are also depicted.

been similar during at least the last 1.5 Ma (Raymo et al., 1998; Venz et al., 1999; Kleiven et al., 2003; Hodell et al., 2008).

In this paper we present new benthic and planktic foraminiferal $\delta^{18}O$ and $\delta^{13}C$ records combined with planktic foraminifer assemblages and ice rafted debris (IRD) data from the subpolar North Atlantic to reconstruct a detailed history of ice sheet growth and determine the impact of major iceberg discharges on surface and deep ocean circulation from ca 800 to 400 ka. At present IODP Site U1314 (Southern Gardar drift, 56°21.8′N, 27°53.3′W, 2820 m water depth, see Fig. 1), is strongly influenced by the North Atlantic current (NAC) and provides an extraordinary opportunity to explore past changes in the surface circulation of the subpolar gyre. The isotopic composition of the water in this area is strongly controlled by the strength of the Iceland Scotland Overflow water (ISOW) (Van Aken and De Boer, 1995; Bianchi and McCave, 2000). Because Site U1314 was drilled deeper than other nearby subpolar North Atlantic sites (ODP 980, 982, 983 or 984) it provides new insight into the mid-Pleistocene deep ocean circulation changes. Moreover, the elevated sedimentation rates of the Gardar Drift (Channell et al., 2006) allow for a detailed comparison of millennial-scale events to nearby records and correlation to ice core data to produce a better understanding of the role of AMOC in climatic variability.

2. Materials and methods

Samples were taken every 4 cm from the composite section made from the 3 cores of Site U1314 (Channell et al., 2006). Each sample was washed with deionized water through a 63 μm mesh to eliminate clay and other fine-grained particles. Samples were then dry-sieved through a 150 μm mesh and separated into two fractions, 63–150 μm and over 150 μm. Census counts and foraminiferal $\delta^{18}O$ and $\delta^{13}C$ analyses were performed on specimens from the coarse fraction.

Benthic foraminiferal stable isotope analyses were performed on an automated carbonate preparation Kiel device I (prototype) coupled to a Finnigan MAT 251 mass spectrometer at the Leibniz laboratory for radiometric dating and Isotope research, in the University of Kiel. Analytical precision based on international standards NBS-19 and NBS-20 was better than 0.07 ‰ for $\delta^{18}O$ and better than 0.05 ‰ for $\delta^{13}C$. Results are reported on the Vienna Pee Dee Belemnite (VPDB) standard scale (Coplen, 1996). *Cibicidoides* (mainly *C. wuellerstorfi*, but sometimes *C. pachyderma* or other *Cibicidoides* spp) were picked for the benthic stable isotope analyses. During a few short intervals where *Cibicidoides* were absent, *Melonis pompilioides* were picked. Between 1 and 8 specimens of *Cibicidoides* larger than 300 μm (most were between 300 and 600 μm) were analyzed. In the case of *M. pompilioides* about 6 specimens were analyzed from the same size fraction as *Cibicidoides*.

Planktic stable isotope analyses were carried out using a Finnigan MAT 252 mass spectrometer at the University of Barcelona. Analytical precision based on the international standard NBS-19 was better than 0.06‰ for $\delta^{18}O$ and reported on the VPDB standard scale. The planktic stable isotope record was based on the subpolar foraminifer *Neogloboquadrina pachyderma* dextral (dex). On average 12 specimens of *N. pachyderma* dex from the 250–300 μm fraction were picked from every other sample. The resolution of the planktic record is the same resolution as for planktic foraminifer census counts.

Prior to isotopic analyses, the selected specimens of each sample were gently crushed between two glass slides under the stereomicroscope to open chambers and facilitate cleaning. The crushed shell fragments were sonicated for 20 s in methanol to eliminate clays and other contaminating particles. Finally, the methanol was removed and samples were air-dried overnight into the gas hood to avoid contamination.

For the planktic foraminifer census counts each sample was split multiple times until the remaining aliquot contained roughly 400 planktic foraminifer specimens (300 at minimum). Mean annual sea surface temperature (SST) at 10 m depth was calculated from planktic foraminifer assemblages using a transfer function based on a back propagating artificial neural network (ANN) (Malmgren et al., 2001) trained on the MARGO (Multiproxy Approach for the Reconstruction of the Glacial Ocean surface) North Atlantic dataset (Kucera et al., 2005). The same set of 10 neural networks as in Kucera et al. (2005) was used in this study, providing 10 different mean annual SST reconstructions. The average values of these 10 temperatures were used for the final reconstruction. The average standard deviation (StDev), also based on the 10 reconstructions, was used to determine how well fossil samples were represented in the calibration dataset (Kucera et al., 2005). Additionally, in order to calculate a similarity index and corroborate the ANN results, we applied a Modern Analog Technique (MAT, Prell, 1985) on the fossil data using the same MARGO modern dataset as was used for the training of the ANNs (Kucera et al., 2005).

3. Results

3.1. Chronological framework

The age model for the studied section (Fig. 2) is based on a correlation of our benthic $\delta^{18}O$ record with the global benthic oxygen isotope stack from Lisiecki and Raymo (2005) (hereafter

Table 1
Tie points used in the correlation between U1314 benthic $\delta^{18}O$ and the global benthic $\delta^{18}O$ stack LR04. Between tie points ages were calculated by linear interpolation.

Site U1314 depth (m)	LR04 time (ka)
32.8	403
33.72	412
35.3	424
35.46	426
35.62	433
36.77	463
37.29	474
37.81	481
38.75	491
40.41	513
42.77	531
43.01	535
44.53	553
44.83	561
45.35	568
45.97	575
46.73	583
47.09	586
47.79	592
48.15	599
49.13	610
49.73	614
50.79	628
51.11	636
51.35	640
52.09	662
52.45	674
53.23	686
53.71	690
55.4	708
55.86	714
56.46	724
57.12	740
57.4	746
58.08	756
58.32	760
58.7	764
59.98	774.8

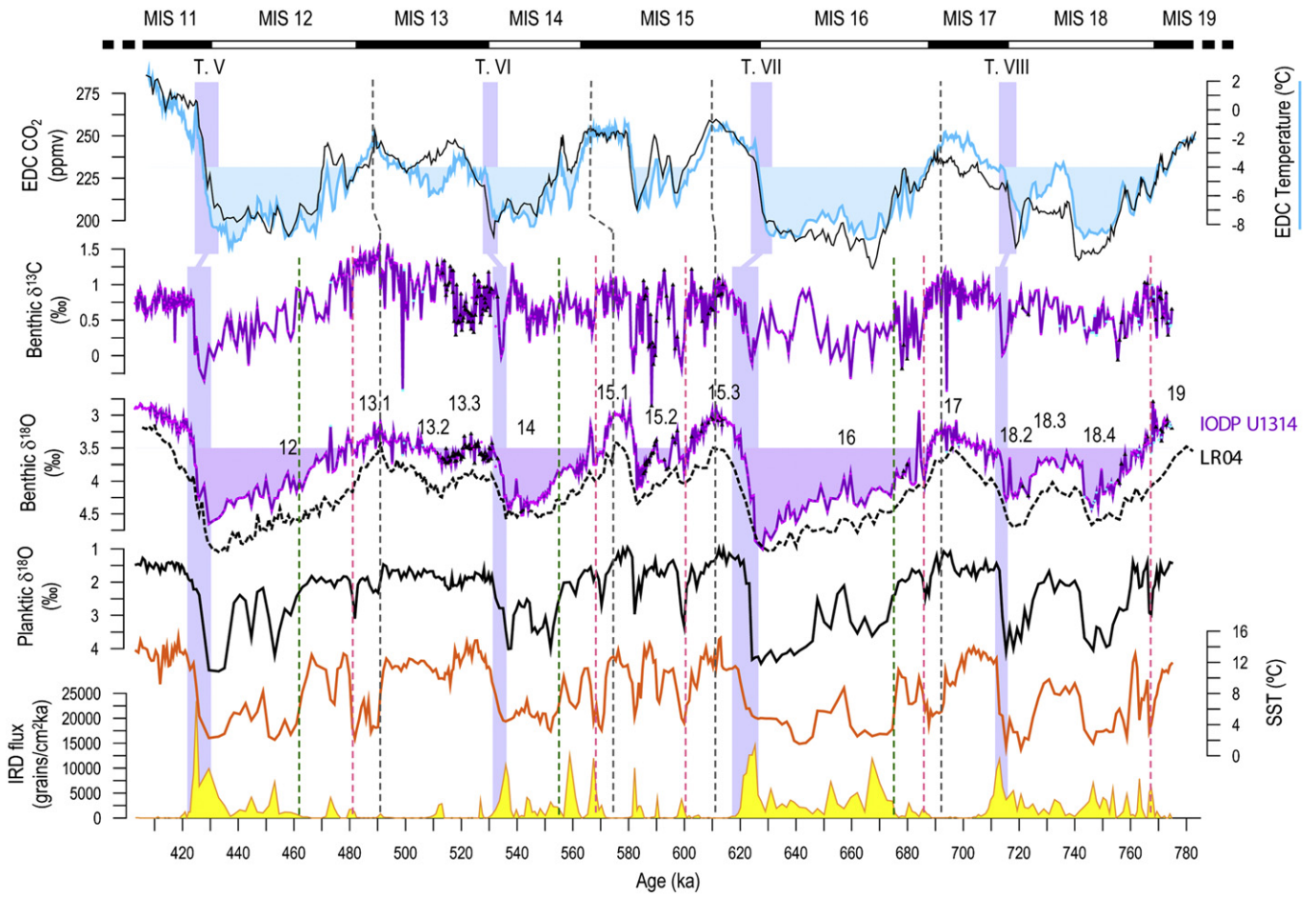

Fig. 3. IODP U1314 records from ca 800 to 400 ka compared with the LR04 benthic $\delta^{18}O$ stack (Lisiecki and Raymo, 2005) and correlated with EPICA Dome C (EDC) temperature and CO_2 records (Siegenthaler et al., 2005; Jouzel et al., 2007; Luthi et al., 2008). From top to bottom: EDC temperature (blue line) and CO_2 (black line) records, DT is filled up to −4 °; Site U1314 benthic $\delta^{13}C$ (purple line); Site U1314 benthic $\delta^{18}O$ (purple line) and LR04 benthic $\delta^{18}O$ stack (black dashed line), U1314 record is filled up to 3.5‰; U1314 planktic $\delta^{18}O$ record of *N. pachyderma* dex (black line); sea surface temperature (SST) reconstruction based on planktic foraminifer census counts from Site U1314 (orange line); IRD fluxes from Site U1314 (orange line filled in yellow). Marine Isotope Stages (MIS) are shown at the top of the figure (glacials in white and interglacials in black) following LR04 ages and substages are indicated with numbers above benthic $\delta^{18}O$. In the benthic stable isotope records the black triangles represent the analyses performed on *Melonis pompilioides*, the pink dots represent *Cibicidoides wuellerstorfi* and the blue dots *Cibicidoides* spp. Terminations are depicted with light violet vertical bars and roman numbers from V to VIII. Vertical grey dashed lines depict glacial inceptions (benthic $\delta^{18}O$ inflections), vertical red dashed lines depict when the thermohaline circulation became disturbed and vertical green dashed lines show the decreases to glacial values in the planktic $\delta^{18}O$ record. (For interpretation of the references to colour in this figure legend, the reader is referred to the web version of this article.)

LR04). *Analyseries* software (Paillard et al., 1996) was used to identify the 38 tie points used for the correlation between records (see Fig. 2 and Table 1).

To constrain accurate ages of the youngest and oldest samples, we compared the Site U1314 benthic $\delta^{18}O$ record with other North Atlantic records. As the first sample records full interglacial conditions, with regard to benthic $\delta^{18}O$ values and SST, within Marine Isotope Stage (MIS) 11 (Figs. 3 and 4), the age of this sample must be at least prior to the beginning of the climate deterioration dated at 398–396 ka (de Abreu et al., 2005; Stein et al., 2009). Additionally, our record presents a cold event in early MIS 11 (represented by a subtle decrease in SST at 33.72 cm mcd, see Figs. 3 and 4) that can be correlated with the cold event recorded in the high resolution record of IODP Site U1313 (Stein et al., 2009) around 412 ka. The Brunhes-Matuyama paleomagnetic transition at 59.1 mcd (Channell et al., 2006) with an average age of ~773.1 ka (Channell et al., 2010) was helpful at establishing a tie point for the oldest samples. However, the age of the Brunhes-Matuyama transition is still controversial depending on the method used to measure the mean point of the transition (Channell et al., 2010; Suganuma et al., 2010).

Sedimentation rates based on this chronology show relatively muted changes (Fig. 2), although it is worth mentioning that during glacial periods the rates were lower than during interglacials, and within the interglacial periods the sedimentation rates were generally higher at the beginning. The mean sedimentation rate was 7.31 cm/ka, in agreement with the rate determined during Expedition 306 for the first 115 mcd (Channell et al., 2006). The lowest sedimentation rates occurred during glacial periods 12 and 16. According to the age model displayed here, the resolution between samples is on average 547 years for the full resolution records and 1094 years for the every other sample records.

3.2. Stable isotopes from planktic and benthic foraminifers

The benthic $\delta^{18}O$ record (Figs. 2 and 3) exhibits four glacial–interglacial cycles with values ranging from 2.8 to 5‰: MIS 13–12 (Fig. 4), MIS 15–14 (Fig. 5), MIS 17–16 (Fig. 6) and MIS 19–18 (Fig. 7). The benthic $\delta^{18}O$ record of Site U1314 and the global isotope stack LR04 indicate that between 800 and 400 ka the largest northern Hemisphere ice sheets developed during MIS 12 and 16

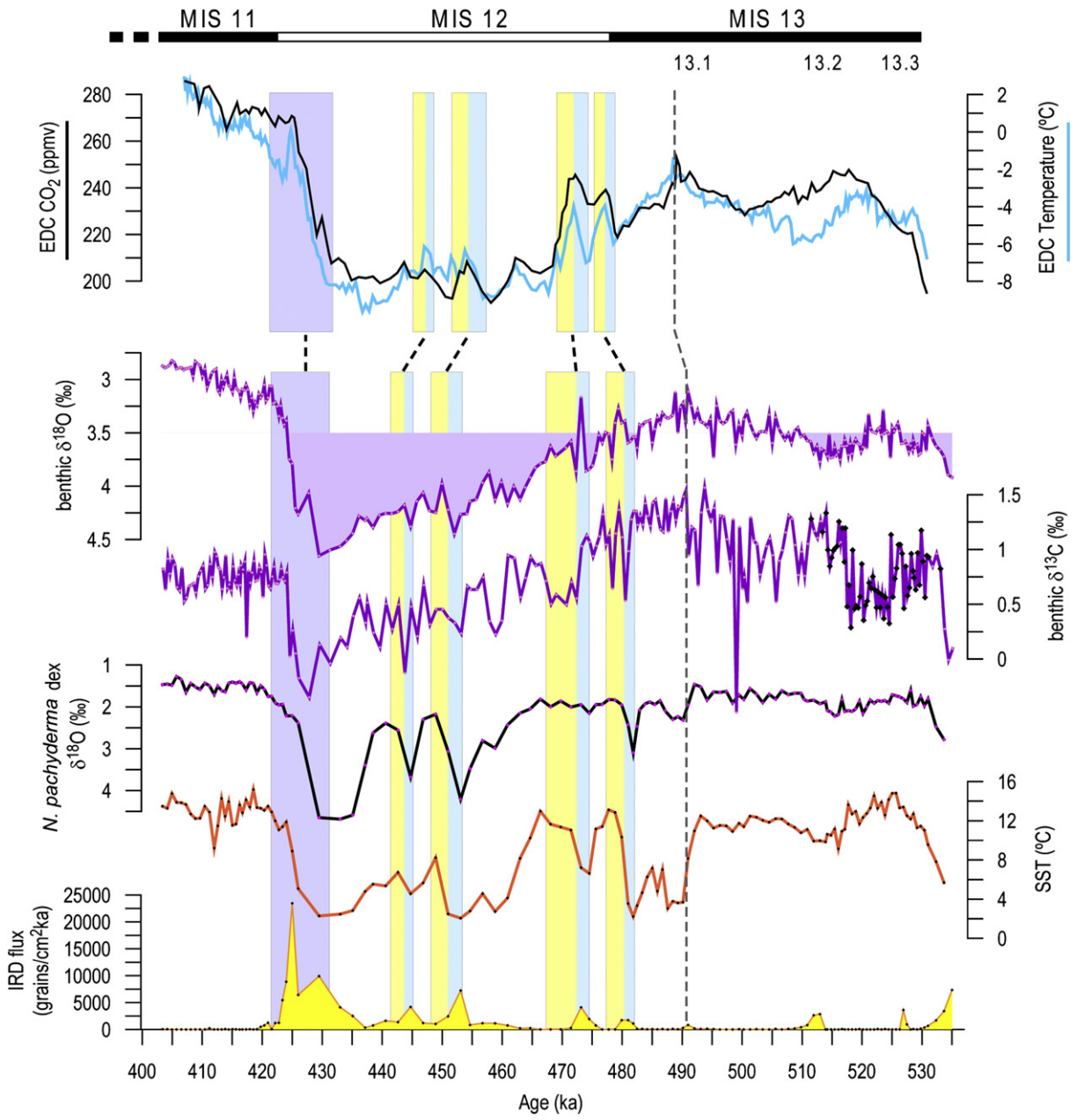

Fig. 4. MIS 11–13 climatic cycle records. From top to bottom: EDC CO_2 record (black) and EDC temperature record (blue); Site U1314 benthic $\delta^{18}O$ record; Site U1314 benthic $\delta^{13}C$ record (black dots represent *M. pompilioides* and pink dots represent *Cibicidoides*, mainly *C. wuellerstorfi*); *N. pachyderma* dex $\delta^{18}O$ record of Site U1314; sea surface temperature (SST) at Site U1314 based on planktic foraminifer census counts; IRD fluxes from Site U1314. Marine Isotope Stages (MIS) and substages are shown for reference at the top of the figure. Vertical bars indicate millennial-scale events, in blue the ice-rafting event and in yellow the associated warming event. Vertical grey dashed lines indicate glacial inceptions. Terminations are shown with vertical light violet bars. (For interpretation of the references to colour in this figure legend, the reader is referred to the web version of this article.)

(Fig. 3), which were the coldest and longest glacial periods, lasting ~53 and ~63 kyr, respectively, whereas MIS 14 and 18 were milder.

The benthic $\delta^{13}C$ record (Fig. 3) exhibits values ranging from −0.35 to 1.5‰. While *C. wuellerstofi* is one of the best recorders of bottom waters $\delta^{13}C$ and was used for most analyses in this study, *M. pompilioides* is a mid-depth infaunal species (Duplessy et al., 1984; Corliss, 1985; McCorkle et al., 1990) and $\delta^{13}C$ results based on this species should be carefully interpreted. In order to adjust *M. pompilioides* results to those of *C. wuellerstofi* we calculated the $\delta^{13}C$ difference between species in 61 samples where both species were analyzed. The average difference was used to adjust both records, −0.12 ‰ for the oxygen and +0.61 ‰ for the carbon isotopes. Our factors are similar to those used in Shackleton and Hall (1984). The adjusted results of *M. pompilioides* were compared with the sparse results of *C. wuellerstofi* during these intervals to check the accuracy of the adjustment. The results presented here follow the same trends as other North Atlantic $\delta^{13}C$ curves like ODP 980 (Flower et al., 2000) and ODP 983 (Kleiven et al., 2003; Raymo et al., 2004) and suggest that *M. pompilioides* results are similar to those obtained with *C. wuellerstofi* in other sites. The sharpest changes in benthic $\delta^{13}C$, with amplitudes between 0.5 and 1‰, were recorded at the beginning of glacial periods, particularly in MIS 15.2 (Figs. 3 and 5), and at Terminations.

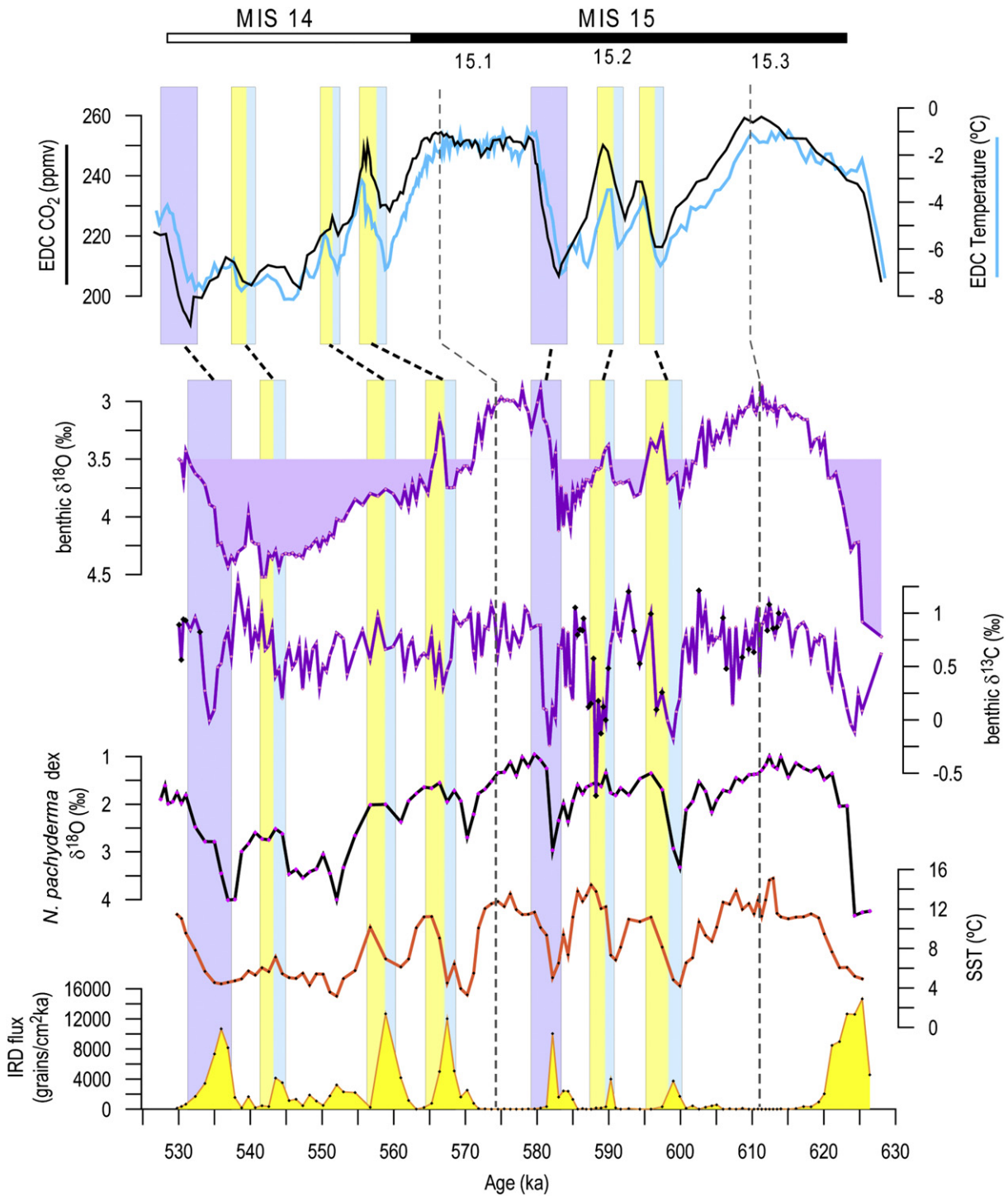

Fig. 5. MIS 14–15 climatic cycle records. See Fig. 4 caption for details. (For interpretation of the references to colour in this figure legend, the reader is referred to the web version of this article.)

N. pachyderma dex $\delta^{18}O$ values range from 1 to 4.7‰. The main trends in this record are similar to those of the benthic $\delta^{18}O$ record although the *N. pachyderma* dex $\delta^{18}O$ record presents a remarkable increase after the first millennial-scale events of every glacial period. The largest amplitude changes were found during millennial-scale ice-rafting events and at terminations, with differences up to 3.1‰. Terminations were more abrupt in the planktic $\delta^{18}O$ record than in the benthic.

3.3. SST reconstruction

The reconstructed mean annual SST was relatively stable during interglacial periods, around 12 °C. This temperature is slightly warmer than the modern SST recorded at this site (~10 °C) according to the World Ocean Atlas data (Locarnini et al., 2006). During glacial periods temperatures were on average much lower, approximately 4 °C. Rapid temperature shifts towards cold SSTs

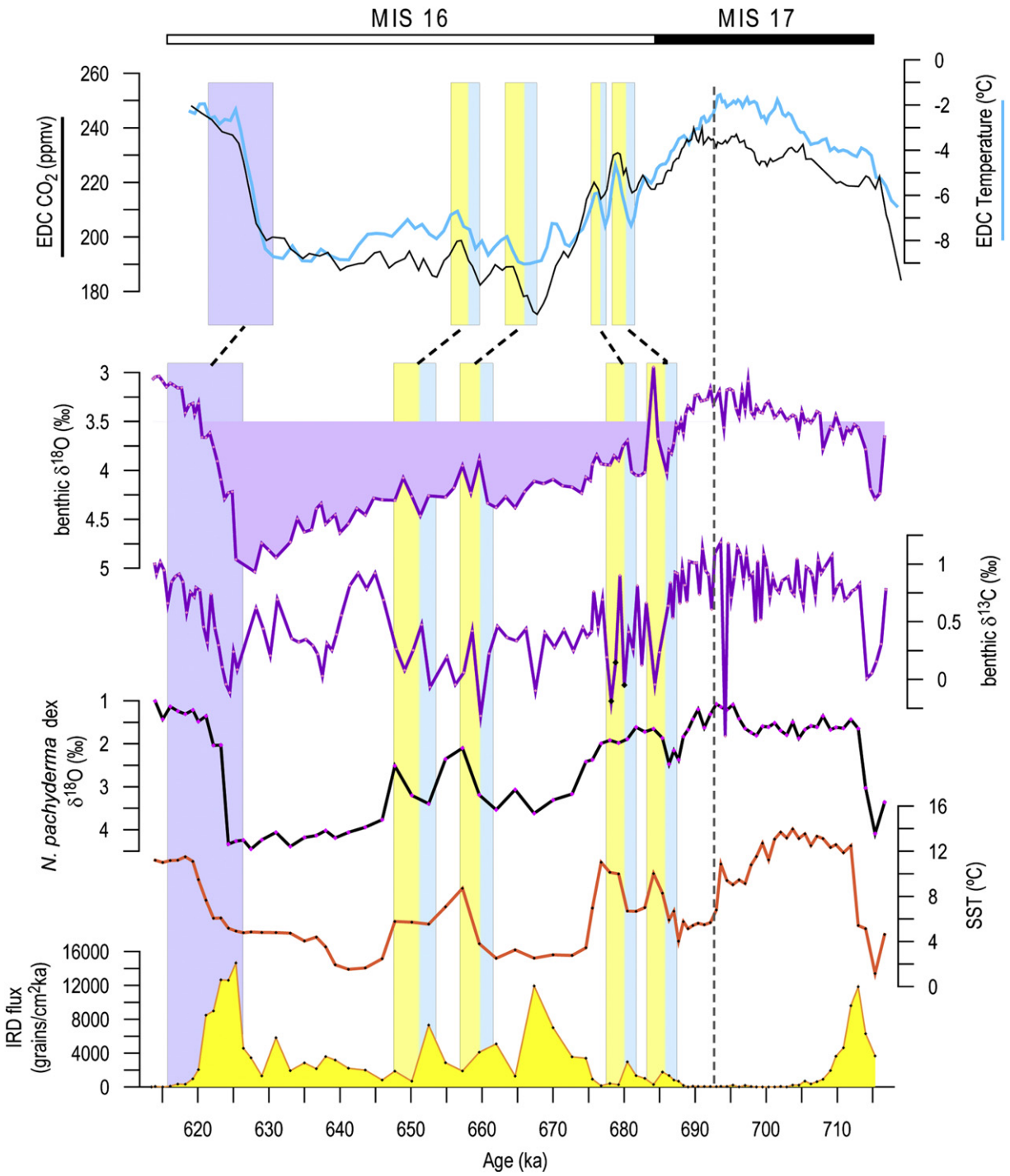

Fig. 6. MIS 16–17 climatic cycle records. See Fig. 4 caption for details. (For interpretation of the references to colour in this figure legend, the reader is referred to the web version of this article.)

(6–10 °C in less than 7 kyr) can be observed in the transition from interglacial to glacial periods (Figs. 4–7). Moreover, during the glacial periods SST shifts of 6–10 °C in ~3 kyr can be observed at millennial-scale warmings.

Standard deviation of the calculated SST was low throughout the record (generally below 0.5 °C) and is poorly correlated with temperature ($R^2 = 0.1325$, see Fig. 8), suggesting that the planktic foraminifer assemblages in the analyzed fossil samples are well represented in the modern dataset and that SST reconstructions are not affected by no-analog artefacts (Kucera et al., 2005). This conclusion is supported by the high values of the similarity index of MAT, above 0.9 for most of the samples (Fig. 8).

3.4. IRD record

Although Site U1314 is located outside the main IRD belt, as defined by Ruddiman (1977), IRD fluxes in the studied section reached values up to 24,000 grains/cm^2 ka and the average size of IRD was up to 0.5 cm. Ice-rafting events (Fig. 3) were more frequent during glacial stages and the highest fluxes were usually associated

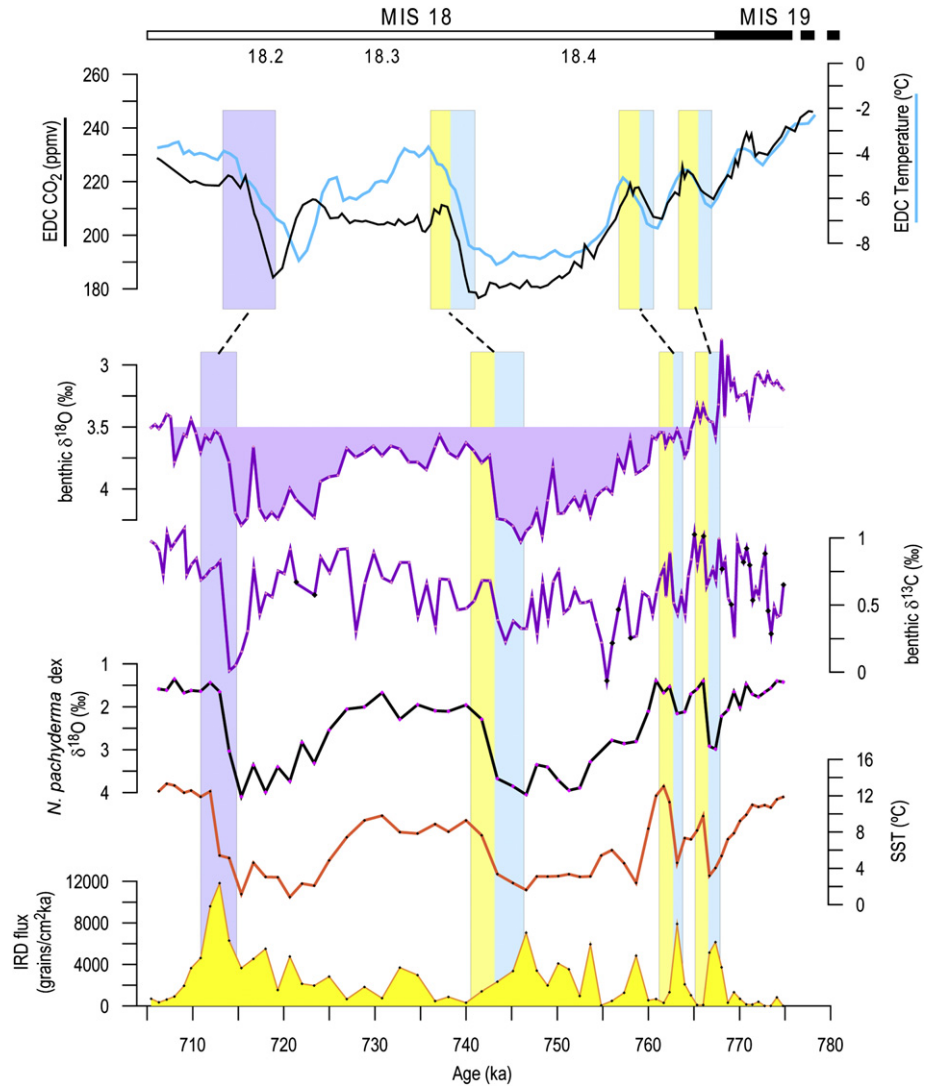

Fig. 7. MIS 18–19 climatic cycle records. See Fig. 4 caption for details. (For interpretation of the references to colour in this figure legend, the reader is referred to the web version of this article.)

with Terminations. The most abundant lithic fragments were quartz and feldspar (including hematite stained grains) and volcanic rock fragments (including volcanic glass).

4. Discussion

4.1. North Atlantic circulation during glacial initiations

After glacial terminations, the benthic $\delta^{18}O$ values remained low during the interglacial periods reflecting low ice volume and hence, warm climate. An inflection in the benthic $\delta^{18}O$ record towards positive values marks the onset of a new glacial period or glacial inception (indicated by vertical grey dashed lines in Figs. 3–7). Several thousands of years after the glacial inception, the benthic $\delta^{13}C$ values in Site U1314 still remained high indicating strong deep water formation in the NGS. Positive benthic $\delta^{13}C$ values were also observed during the first kyr of glacial initiations in the eastern North Atlantic Site 980 (McManus et al., 1999; Wright and Flower, 2002) which was interpreted as a persistent North Atlantic deep water (NADW) production called 'lagging NADW production' (Wright and Flower, 2002). Because isotopic composition of the deep water at Sites U1314 and 980 is strongly controlled by the ISOW, the high benthic $\delta^{13}C$ values observed at glacial initiations (Fig. 9) suggest that the deep water formation in the NGS was still not disturbed. Furthermore, each glacial initiation was associated with a pronounced sea surface cooling with a SST change of 6–10 ° in less than 7 kyr. Similar changes in temperature can be inferred from ODP Sites 646, 647 and 984 data, west and north of Site U1314, where percentages of *N. pachyderma* sininstral increased rapidly (Aksu et al., 1989; Wright and Flower, 2002). However, Site 980 located at similar latitude to Site U1314 but in the eastern part of the North Atlantic, exhibits that SSTs remained warm after glacial inceptions (McManus et al., 1999; Wright and Flower, 2002), known as 'lagging warmth' of glacial initiations (Wright and Flower, 2002). Thus, the cooling observed in Site U1314 may not be a widespread feature of the North Atlantic but rather restricted to the high latitudes of the western North Atlantic.

A similar display of warm SSTs restricted to the eastern part of the subpolar North Atlantic and high benthic $\delta^{13}C$ values was described for the interglacial to glacial transition of the last climatic cycle (Ruddiman and McIntyre, 1979; Ruddiman et al., 1980; Chapman and Shackleton, 1999; Oppo et al., 2001, 2006; McManus et al., 2002). The persistent warm temperatures in the eastern North Atlantic during glacial initiations were attributed to

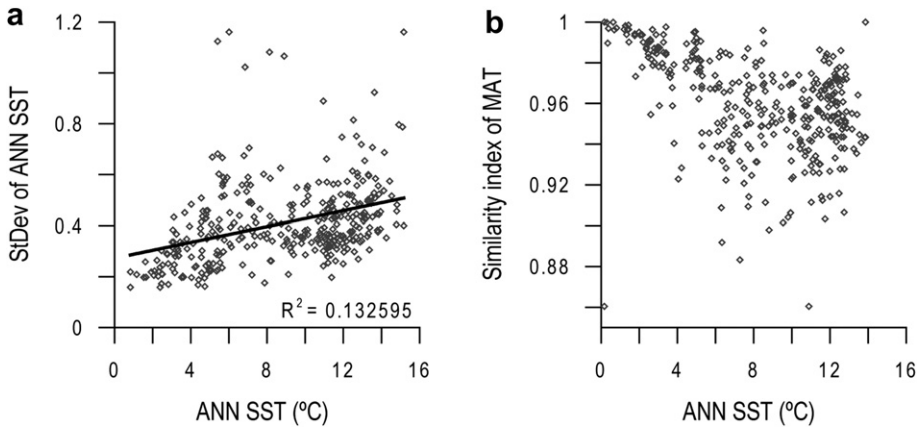

Fig. 8. Cross-correlation between the sea surface temperature calculated with artificial neural networks (ANN SST) and their standard deviation (a), and between the ANN SST and the similarity index of modern analog technique (MAT) (b). The low correlation coefficient (R^2) and the high similarity index indicate that the studied samples are well represented in the modern dataset and the temperatures calculated are not biased by no-analog situations.

the continuous flow of the NAC, which still flowed towards the Norwegian Greenland Sea (NGS) and maintained active deep water formation (Ruddiman and McIntyre, 1979, 1981; Ruddiman et al., 1980; McManus et al., 2002; Risebrobakken et al., 2007). These authors suggest that during the Last Glacial initiation the continuous flow of the NAC promoted the transport of moisture from low to high latitudes, creating an optimal configuration for rapid ice sheet growth. The rapid increase in the benthic $\delta^{18}O$ record of Site U1314 after glacial inceptions suggests that the glacial initiations between 800 and 400 ka were also characterized by

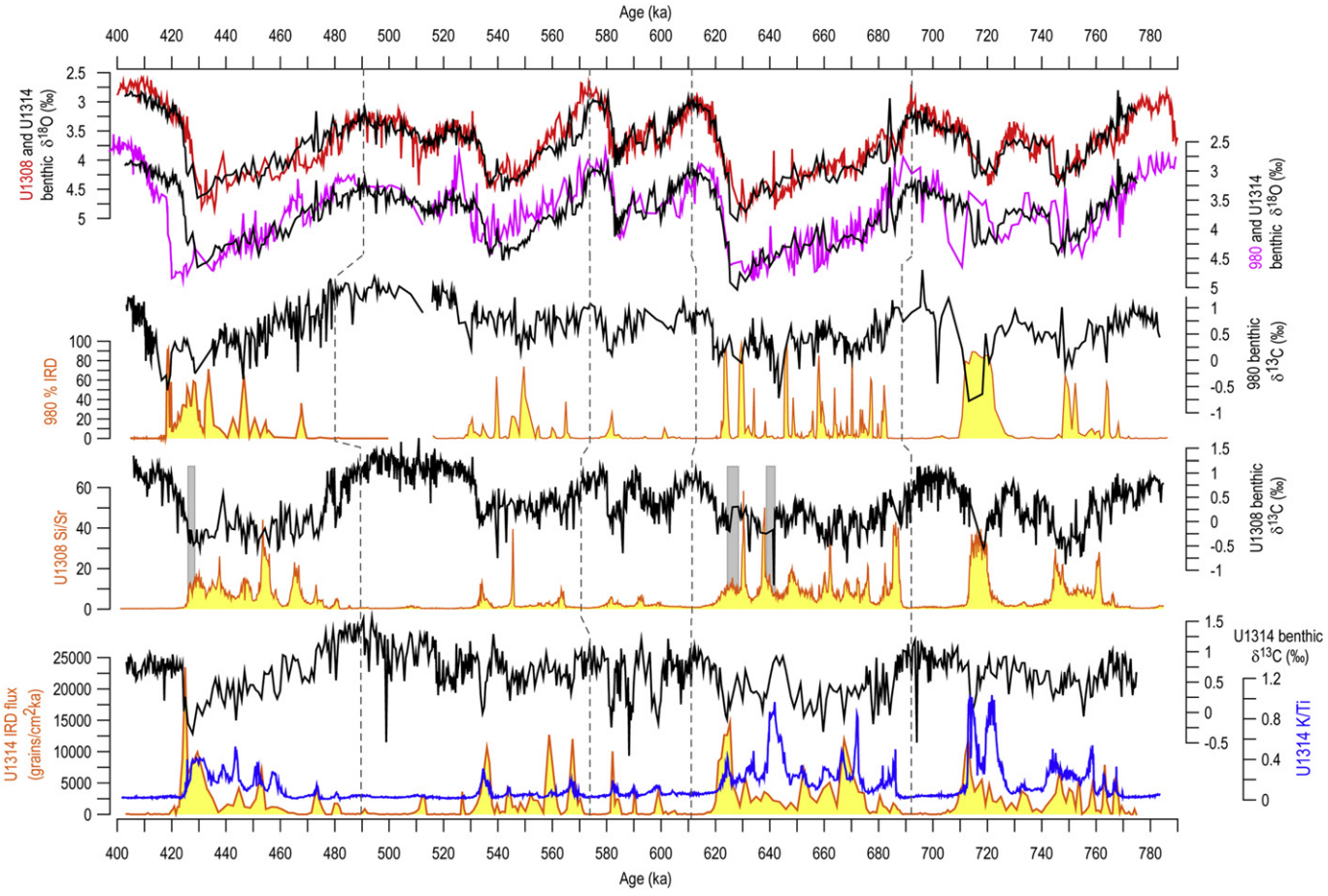

Fig. 9. Comparison between benthic $\delta^{13}C$ and IRD records of the North Atlantic sites ODP 980 at 2179 m depth (McManus et al., 1999; Wright and Flower, 2002), IODP U1308 at 3427 m (Hodell et al., 2008) and IODP U1314 at 2820 m (this study). The chronologies of sites 980 and U1308 datasets are the same as in the original publication. Benthic $\delta^{18}O$ records of Site U1308 and Site 980 are plotted versus benthic $\delta^{18}O$ of Site U1314 in order to see the similarity between the age models of every record. IRD proxies (orange line filled in yellow) of each site are plotted versus their benthic $\delta^{13}C$ records (black). In the IRD record of U1308 vertical grey bars show the 'Hudson Strait Heinrich events' found by Hodell et al. (2008). The K/Ti record of Site U1314 (blue line) (Grützner and Higgins, 2010) shows the strong correlation between ice-rafting and the strength of the ISOW (represented by K/Ti ratios). (For interpretation of the references to colour in this figure legend, the reader is referred to the web version of this article.)

a dominant transfer of freshwater from the ocean to the continents leading to rapid ice sheet growth in the Northern Hemisphere. Temperature decreases in the western North Atlantic at glacial initiations may indicate that cold and low salinity waters spread southwestwards due to a higher ice export through the East Greenland current (EGC). The presence of IRD at Site U1314 (Figs. 4–7) which coincides with the SST decrease supports the occurrence of small scale ice-rafting events and/or a higher sea ice export to the subpolar gyre. The presence of cold low salinity water in the western North Atlantic might have reduced deep water formation in the Labrador Sea as suggested for the Last Glacial inception in a recent model study (Born et al., 2010). Moreover, fresh water input to the subpolar gyre surface waters may have reduced regional convection and reorganized North Atlantic surface circulation (Hatun et al., 2005; Born et al., 2010). According to Born et al. (2010), if the subpolar gyre was weakened, less salt would be advected into the Labrador Sea and more into the NGS. As a result, deep water convection in the NGS would be similar or slightly higher but the overall AMOC would be reduced by approximately 15%. The 'lagging NADW production' identified in the path of the ISOW by the high benthic $\delta^{13}C$ values, probably was concealing the fact that, as the ice sheets grew, the AMOC was slightly reduced due to the loss of deep water convection in the western North Atlantic. We advocate that the cooling and freshening of the western part of the North Atlantic may have been an important factor in the development of glacial periods through the reduction of one of the components of the AMOC.

4.2. Ice-rafting events and millennial-scale climatic variability

The flux of IRD to the southern Gardar drift was nearly zero during most of the interglacial periods studied (Fig. 3). Consistent with the data from Site 980 (McManus et al., 1999), the major ice-rafting events at Site U1314 always occurred when the 3.5‰ threshold in the benthic $\delta^{18}O$ was surpassed. Although changes in benthic $\delta^{18}O$ are driven by deep water temperature and ice volume (Shackleton, 1987), this 3.5‰ threshold must represent the conditions when the ice sheets were large enough to undergo instabilities and produce major ice-rafting events. Thereby, the ice sheet growth, which started during glacial inceptions, was not interrupted for several thousand years until the ice sheets were large and unstable. For instance, between the glacial inception at MIS 13/12 transition (~492 ka, grey dashed line in Fig. 4) to the first significant ice-rafting event (~481 ka), there was a ~11 kyr interval in which the ice sheet growth was continuous. A similar lag is observed in MIS 15.1/14, MIS 15.3/15.2, and MIS 17/16 transitions (Figs. 5 and 6).

The lack of dolomite and limestone in Site U1314 IRD, which is very abundant in the main IRD belt (Heinrich, 1988; Bond et al., 1992; Hemming, 2004), suggests that North America was not the main source of icebergs for this region, even at the time of the 'Hudson Strait Heinrich events' described at Site U1308 (Hodell et al., 2008, see Fig. 9) or the "Heinrich-like events" identified in Site U1313 (Stein et al., 2009). The abundance of quartz, feldspar and volcanic glass in the IRD and the regional Atlantic surface circulation argue in favor of Greenland and Iceland as the main source of the icebergs that reached Site U1314, although a Scandinavian or Svalbard origin is also possible (Bond and Lotti, 1995; Hemming et al., 1998; Bond et al., 2001; Moros et al., 2004).

The ice-rafting events occurred during cold intervals and were immediately followed by negative excursions in the benthic $\delta^{18}O$ (approximately between 0.25 and 1.5‰, see Figs. 4–7) and $\delta^{13}C$ (approximately between 0.5 and 1‰), and also by abrupt warmings (6–10 °C in ~3 kyr). Since the icebergs that reached Site U1314 mainly came from Greenland, Iceland and Scandinavia, this first pulse of iceberg discharges may have caused a freshening of the NGS decreasing deep water convection. Because Site U1314 is near the Iceland Scotland Ridge, it is possible that benthic $\delta^{13}C$ values at Site U1314 were depleted as a result of either a higher influence of the poorly ventilated nutrient enriched waters of the SOW (Oppo and Fairbanks, 1987; Curry et al., 1988; Duplessy et al., 1988; Oppo and Lehman, 1993; Oppo et al., 1995) or because of the influence of the NGS overflows of deep water generated by brine rejection (Raymo et al., 2004; Yu et al., 2008) or a mixture of both sources. Whatever the origin, the reduction in the $\delta^{13}C$ values indicates a reduction in the deep water convection in the NGS and, hence, in the generation of ISOW. The reduction in the ISOW at ice-rafting events is also supported by the K/Ti record of Site U1314 (Grützner and Higgins, 2010). Low K/Ti ratios have been interpreted as enhanced transport of basalt-derived titanomagnetites (high ISOW) whereas high ratios represent the dominance of acidic sediment sources (low ISOW). Fig. 9 illustrates that almost every ice-rafting episode is related to an increase in the K/Ti ratio and a decrease in the benthic $\delta^{13}C$ values.

The negative excursions in the benthic $\delta^{18}O$ record during ice-rafting events suggest that the ice sheets waned and sea level rose due to calving and/or to ice melting, similarly to the sea level rises that occurred during MIS 3 (Siddall et al., 2003, 2008; Rohling et al., 2004, 2008; Arz et al., 2007; Sierro et al., 2009). However, these excursions with average amplitudes of 0.5‰ are too high to be only associated with ice volume, as this would represent a sea level rise of around 50 m. Part of the benthic $\delta^{18}O$ decrease is probably related to deep sea hydrographic changes (Skinner et al., 2003; Skinner and Elderfield, 2007; Yu et al., 2008).

In the studied section glaciations exhibit several millennial-scale SST warmings associated with ice-rafting events. It is remarkable that the first significant pulse of iceberg delivery to the North Atlantic at each glacial period (vertical dashed red lines in Fig. 3) caused a dramatic change in deep water production at the NGS which led to the glacial deep water circulation style. Moreover, the warm interval that followed the first ice-rafting event was very abrupt and near to interglacial SSTs were reached. The first two ice-rafting events of each glacial period were linked to the strongest millennial-scale SST shifts even though the IRD fluxes were not the highest. Rapid warmings at the end of the ice-rafting events might be linked to the destabilization of the halocline established during ice-rafting and rapid upwelling of the warm and salty water stored in the subsurface layer (Moros et al., 2002; Rasmussen and Thomsen, 2004). This hypothesis is supported by the results of several circulation model experiments (Marotzke, 1989; Wright and Stocker, 1991; Winton, 1997; Weaver, 1999; Paul and Schulz, 2002; Mignot et al., 2007) and by other Last Glacial period North Atlantic records (van Kreveld et al., 2000; Peck et al., 2008; Jonkers et al., 2010) which suggested that the NAC flowed below the freshwater lid, caused by the ice-rafting, building up warm and salty waters in the subsurface layer.

After these first two millennial-scale events, the warm intervals ensuing ice-rafting were milder at Site U1314. This finding resembles the threshold at larger ice volumes found at Site 980 (McManus et al., 1999), above which climatic variability was reduced. However, in Site U1314 the amplitude of SST changes was reduced when the benthic $\delta^{18}O$ record of Site U1314 exceeded ~4‰ instead of 4.5–4.6‰. The different thresholds at each site may be linked to their location. As the AMOC reduced NAC weakened, and during the next ice-rafting events either less warm water was stored in the subsurface layer or it was stored southeastwards. As a result, the millennial-scale warm events might be milder at Site U1314 earlier than in Site 980.

The ice-rafting events observed in MIS 15.2 (Fig. 5) are particularly outstanding because they were linked to the strongest oscillations in the benthic $\delta^{13}C$, with the exception of the

terminations. These benthic $\delta^{13}C$ oscillations were also recorded in other North Atlantic sites like 980 (Wright and Flower, 2002) and 983 (Raymo et al., 2004) but in Site U1314 they presented a higher amplitude (Fig. 9). It is likely that the location of U1314 makes this site extremely sensitive to changes in the production of the ISOW and the shoaling of SOW whereas Site 980 recorded shallower changes in the water masses. The benthic $\delta^{13}C$ record of Site 983, also in the path of the ISOW, shows 3 abrupt shifts that can be correlated with the benthic $\delta^{13}C$ oscillations in Site U1314 supporting the idea that strong changes in the ISOW production occurred during MIS 15.2, although the resolution of this record is much lower for this interval. The analysis of Site U1314 records suggests that during MIS 15.2 the depth of the chemocline which separates the ISOW from the SOW shifted rapidly linked to strong dampenings and rejuvenations of the ISOW due to calving and meltwater discharges to the NGS.

4.3. Planktic $\delta^{18}O$ record versus SST

After glacial inceptions, *N. pachyderma* dex $\delta^{18}O$ values were relatively low with respect to the glacial values and only shows brief positive excursions related to the ice-rafting events (Figs. 3–7). The census counts indicate cold mean annual SSTs (below 6 °) during glacial initiations but the *N. pachyderma* dex $\delta^{18}O$ values remained rather low. At present, *N. pachyderma* dex preferably inhabits the top 50–100 m, associated with the thermocline and deep chlorophyll maximum and it has been related to the warm and stratified surface waters of the summer-autumn in the Northeast Atlantic and the NGS (Fairbanks et al., 1982; Reynolds-Sautter and Thunell, 1989, 1991; Schiebel and Hemleben, 2000; Schiebel et al., 2001; Nyland et al., 2006; Chapman, 2010). Following recent interpretations of planktic $\delta^{18}O$ changes in sites near U1314 (Hodell et al., 2010; Jonkers et al., 2010), we attributed the low *N. pachyderma* dex $\delta^{18}O$ values mostly to warmer summer temperatures driven by the higher influence of the North Atlantic Drift at Site U1314 during the summer. In this context, during the summers of glacial initiations the warm waters of the NAC still reached Site U1314 area and this may have introduced heat and moisture into the subpolar gyre promoting snow accumulation in North America and the areas surrounding the subpolar gyre.

During ice-rafting events, *N. pachyderma* dex $\delta^{18}O$ record exhibits positive excursions probably linked to low summer SSTs driven by the ice-rafting. Planktic $\delta^{18}O$ values decreased rapidly when the ice rafting declined and low $\delta^{18}O$ values were reached before the mean annual SST increased near to interglacial values. A similar phase relationship between ice-rafting and planktic $\delta^{18}O$ has been described in other North Atlantic sites (Elliot et al., 1998; Moros et al., 2002; Hodell et al., 2010; Jonkers et al., 2010). This early warming has been associated with the presence of a subsurface warm layer that shoaled seasonally during the summer (Moros et al., 2002; Rasmussen and Thomsen, 2004; Jonkers et al., 2010), which is consistent with our results because *N. pachyderma* dex lives preferably during the summer. The shift to high *N. pachyderma* dex $\delta^{18}O$ values occurred after the first two millennial-scale events (green dashed lines in Fig. 3) and was rather abrupt (4–10 ka). If attributed mostly to temperature, it seems that summer temperatures turned cold only when the AMOC was severely reduced and the warm water of the NAC could not reach Site U1314 even during the summer.

4.4. Comparison with the Antarctic ice core records and phasing between surface and deep water proxies

Shackleton et al. (2000) observed a strong similarity between the benthic $\delta^{18}O$ record and the deuterium temperature of the Antarctic ice cores during the Last Glacial period. Our benthic $\delta^{18}O$ record and the EPICA Dome Concordia (EDC) deuterium temperature record are also very similar (Figs. 3–7), and most of the cold and warm intervals can be correlated with benthic $\delta^{18}O$ changes. It is striking that the first two millennial-scale warm events observed in the North Atlantic Site U1314 were also observed as high amplitude warming events in not only Antarctic temperature but also CO_2. Furthermore, other less prominent warm millennial-scale events can be also recognized in EDC records. This strong correlation between Northern and Southern Hemisphere records argues in favour of a strong climatic coupling between both hemispheres.

The chronology of LR04 differs several kyr from the age model EDC3 (Parrenin et al., 2007) but the difference between both age models is not constant. Thus, constraining the phase relationship between the events recorded in the Northern Hemisphere records and their counterparts in the Southern Hemisphere is not possible. Determining phase relationships between both hemispheres is challenging beyond the Last Glacial period because the methane records of Greenland, which have been used to synchronize the records of both hemispheres, only spanned up to MIS 5 (Blunier et al., 1998; Blunier and Brook, 2001; Ahn and Brook, 2008). However, we may compare the surface records of Site U1314 (SST, planktic oxygen isotopes and IRD) to the benthic oxygen isotopes of the same site, assuming that the benthic $\delta^{18}O$ was synchronous with the Antarctic temperature signal like during the last climatic cycle (Shackleton et al., 2000; Skinner et al., 2003). A similar strategy was used in Hodell et al. (2010) and Channell et al. (2010). Most of the benthic $\delta^{18}O$ negative shifts have their counterpart events in the SST record, but SST slightly lags benthic $\delta^{18}O$ (Figs. 4–7). Since the benthic $\delta^{18}O$ represents the Antarctic temperature, Northern Hemisphere SSTs lagged Antarctic temperatures. The *N. pachyderma* dex $\delta^{18}O$ record does not show this lag with respect to benthic $\delta^{18}O$ because this record represents summer temperatures (see Section 4.3) and it has been shown that during the Last Glacial period summer temperatures were warm during the late ice-rafting events due to the shoaling of subsurface warm waters (Moros et al., 2002; Jonkers et al., 2010). However, the coupling between surface and deep water proxies at Site U1314 strongly supports a narrow coupling between both hemispheres at the millennial timescale. The phasing between SST and the Antarctic temperatures (represented by the benthic $\delta^{18}O$) resembles the "bipolar seesaw" mechanism (Broecker, 1998) that was already observed for the Antarctic warmings and Heinrich events during the Last Glacial period (Blunier et al., 1998; Blunier and Brook, 2001).

5. Conclusions

The study of benthic and planktic stable isotopes, planktic foraminifer assemblages and IRD flux from Site U1314 in the North Atlantic allowed us to reconstruct climate variability during glacial periods at millennial and orbital timescales between 800 and 400 ka.

Glacial initiations started when benthic $\delta^{18}O$ values began to increase and they were characterized by a rapid cooling at Site U1314 (6–10 °C in less than 7 kyr) whereas in the eastern North Atlantic the annual SST remained high during several kyr because the NAC continued flowing towards the NGS (McManus et al., 1999; Wright and Flower, 2002). High benthic $\delta^{13}C$ values at both sites, U1314 and 980, indicate that deep water formation was still vigorous in the NGS. The prevalence of active deep water formation during glacial initiations promoted ice sheet growth in the Northern Hemisphere because the NAC provided moisture to the high latitudes. However, the cold SSTs at Site U1314 suggest a cooling, and probably freshening, of the subpolar gyre, which could have decreased deep water formation in the Labrador Sea

and, hence, moderately reduced the AMOC, according to recent climate models (Born et al., 2010).

During glacial initiations ice sheet growth was continuous and large amounts of freshwater accumulated on the continents. When the ice volume reached certain threshold (3.5‰ in the benthic $\delta^{18}O$) ice-rafting events started and the ice sheet growth was punctuated by millennial-scale events of ice sheet waning. This threshold for ice-rafting has been a constant climatic feature at least for the last 800 ka. The drop in the benthic $\delta^{13}C$ values at Site U1314 during ice-rafting events suggests that the iceberg discharges freshened the subpolar North Atlantic preventing deep water formation. At the end of the iceberg discharges, mean annual SSTs began to increase. The change towards warm conditions was probably caused by the upwelling of warm waters stored in the subsurface layer during ice-rafting events which likely shoaled during the summers when ice-rafting was still active (Moros et al., 2002; Rasmussen and Thomsen, 2004; Jonkers et al., 2010). The first two ice-rafting events at Site U1314 were followed by strong millennial-scale warm events in which mean annual SSTs were similar to interglacial temperatures whereas subsequent millennial-scale warm intervals were milder.

The significant correlation between Site U1314 and EDC records strongly argues in favour of a climatic coupling between both hemispheres although we cannot directly compare them because of their different age models. Nevertheless, mid-Pleistocene phasing between both hemispheres has been inferred comparing the surface ocean proxies with the benthic $\delta^{18}O$ record (which represents the Antarctic signal) of Site U1314. This study highlights the strong similarity of the mid-Pleistocene climatic cycles with the Last Glacial–Interglacial cycle with respect to ice sheet growth at glacial initiations and the millennial-scale variability of glacial periods, even though mid-Pleistocene climate conditions were slightly different. Both hemispheres were closely coupled at millennial timescales over four glacial–interglacial cycles within the 800–400 ka interval. Furthermore, the millennial-scale seesaw pattern, which has been prevalent during the Last Glaciation, also characterized the glacial–interglacial cycles from 800 to 400 ka suggesting a strong linkage between both hemispheres for the last 800 ka.

Acknowledgements

This research used samples provided by the Integrated Ocean Drilling Program, IODP. The map was also provided by IODP (K. Petronotis). Thanks to I. Hernandez-Almeida, B. Flower and C. Williams for their help. We also thank two anonymous reviewers for their useful advices and suggestions which undoubtedly helped us to improve the manuscript. This study was funded by the research projects CGL2005-00642/BTE, CGL2006-10593, CGL2008-05560, as well as the Ministry of Education and Science project GRACCIE (CONSOLIDER-INGENIO CSD 2007-00067) and Junta de Castilla y León fundings (Grupo de excelencia GR34). Support from the Spanish government through a FPU fellowship granted to Montserrat Alonso García is gratefully acknowledged.

References

Ahn, J., Brook, E.J., 2008. Atmospheric CO_2 and climate on millennial time scales during the last glacial period. Science 322, 83–85.

Aksu, A.E., de Vernal, A., Mudie, P.J., 1989. High-resolution foraminifer, palynologic, and stable isotopic records of upper Pleistocene sediments from the Labrador Sea: paleoclimatic and paleoceanographic trends. In: Srivastava, S.P., Arthur, M., Clement, B. (Eds.), Proceedings of the Ocean Drilling Program, Scientific Results, pp. 617–652.

Arz, H.W., Lamy, F., Ganopolski, A., Nowaczyk, N., Pätzold, J., 2007. Dominant Northern Hemisphere climate control over millennial-scale glacial sea-level variability. Quaternary Science Reviews 26, 312–321.

Berger, W.H., Jansen, E., 1994. Mid-Pleistocene climate shift – the Nansen connection. In: Johannessen, O.M., Muench, R.D., Overland, J.E. (Eds.), The Polar Oceans and Their Role in Shaping the Global Environment. AGU, Washington D.C., pp. 295–311.

Berger, W.H., Wefer, G., 2003. On the dynamics of the ice ages: stage-11 paradox, mid-Brunhes climate shift, and 100-ky Cycle. In: Droxler, A.W., Poore, R.Z., Burkle, L.H. (Eds.), Earth's Climate and Orbital Eccentricity. The Marine Isotope Stage 11 Question. Geophysical Monograph, vol. 137. Americal Geophysical Union, Washington D.C., pp. 41–59.

Bianchi, G.G., McCave, I.N., 2000. Hydrography and sedimentation under the deep western boundary current on Björn and Gardar Drifts, Iceland Basin. Marine Geology 165, 137–169.

Blunier, T., Brook, E.J., 2001. Timing of millennial-scale climate change in Antarctica and Greenland during the last glacial period. Science 291, 109–112.

Blunier, T., Chappellaz, J., Schwander, J., Dallenbach, A., Stauffer, B., Stocker, T.F., Raynaud, D., Jouzel, J., Clausen, H.B., Hammer, C.U., Johnsen, S.J., 1998. Asynchrony of Antarctic and Greenland climate change during the last glacial period. Nature 394, 739–743.

Bond, G.C., Lotti, R., 1995. Iceberg discharges into the North Atlantic on millennial time scales during the last glaciation. Science 267, 1005–1010.

Bond, G., Heinrich, H., Broecker, W., Labeyrie, L., McManus, J., Andrews, J., Huon, S., Jantschik, R., Clasen, S., Simet, C., Tedesco, K., Klas, M., Bonani, G., Ivy, S., 1992. Evidence for massive discharges of icebergs into the North Atlantic Ocean during the last glacial period. Nature 360, 245–249.

Bond, G., Broecker, W., Johnsen, S., McManus, J., Labeyrie, L., Jouzel, J., Bonani, G., 1993. Correlations between climate records from North Atlantic sediments and Greenland ice. Nature 365, 143–147.

Bond, G., Kromer, B., Beer, J., Muscheler, R., Evans, M.N., Showers, W., Hoffmann, S., Lotti-Bond, R., Hajdas, I., Bonani, G., 2001. Persistent solar influence on north atlantic climate during the Holocene. Science 294, 2130–2136.

Born, A., Nisancioglu, K., Braconnot, P., 2010. Sea ice induced changes in ocean circulation during the Eemian. Climate Dynamics 35, 1361–1371.

Boyle, E.A., Keigwin, L.D., 1982. Deep circulation of the North Atlantic over the last 200,000 years: geochemical evidence. Science 218, 784–787.

Boyle, E.A., Keigwin, L., 1987. North Atlantic thermohaline circulation during the past 20,000 years linked to high-latitude surface temperature. Nature 330, 35–40.

Broecker, W.S., 1998. Paleocean circulation during the last deglaciation: a bipolar seesaw? Paleoceanography 13, 119–121.

Broecker, W., Bond, G., Klas, M., Clark, E., McManus, J., 1992. Origin of the northern Atlantic's Heinrich events. Climate Dynamics 6, 265–273.

Channell, J.E.T., Kanamatsu, T., Sato, T., Stein, R., Alvarez Zarikian, C.A., Malone, M.J., Scientists, T.E., 2006. 303/306 Expedition Reports, North Atlantic Climate, Proceedings of the Integrated Ocean Drilling Program. Integrated Ocean Drilling Program Management International, Inc., College Station TX.

Channell, J.E.T., Hodell, D.A., Singer, B.S., Xuan, C., 2010. Reconciling astrochronological and 40Ar/39Ar ages for the Matuyama-Brunhes boundary and late Matuyama Chron. Geochemistry Geophysics Geosystems 11, Q0AA12. doi:10.1029/2010GC003203.

Chapman, M.R., 2010. Seasonal production patterns of planktonic foraminifera in the NE Atlantic Ocean: implications for paleotemperature and hydrographic reconstructions. Paleoceanography 25, PA1101. doi:10.1029/2008PA001708.

Chapman, M.R., Shackleton, N.J., 1999. Global ice-volume fluctuations, North Atlantic ice-rafting events, and deep-ocean circulation changes between 130 and 70 ka. Geology 27, 795–798.

Coplen, T.B., 1996. More uncertainty than necessary. Paleoceanography 11, 369–370. doi:10.1029/1096PA01420.

Corliss, B.H., 1985. Microhabitats of benthic foraminifera within deep-sea sediments. Nature 314, 435–438.

Curry, W.B., Lohmann, G.P., 1983. Reduced advection into Atlantic Ocean deep eastern basins during last glaciation maximum. Nature 306, 577–580.

Curry, W.B., Oppo, D.W., 2005. Glacial water mass geometry and the distribution of δ13C of Sigma CO 2 in the western Atlantic Ocean. Paleoceanography 20, 1–12.

Curry, W., Duplessy, J., Labeyrie, L., Shackleton, N., 1988. Changes in the distribution of δ13 C of deep water ΣCO 2 between the Last Glaciation and the Holocene. Paleoceanography 3, 317–341.

de Abreu, L.c., Abrantes, F.t.F., Shackleton, N.J., Tzedakis, P.C., McManus, J.F., Oppo, D.W., Hall, M.A., 2005. Ocean climate variability in the eastern North Atlantic during interglacial marine isotope stage 11: A partial analogue to the Holocene? Paleoceanography 20. doi:10.1029/2004PA001091.

deMenocal, P.B., Oppo, D.W., Fairbanks, R.G., Prell, W.L., 1992. Pleistocene δ13C variability of North Atlantic intermediate water. Paleoceanography 7, 229–250.

Dickson, R.R., Gmitrowicz, E.M., Watson, A.J., 1990. Deep-water renewal in the northern North Atlantic. Nature 344, 848–850.

Duplessy, J.-C., Shackleton, N.J., Matthews, R.K., Prell, W., Ruddiman, W.F., Caralp, M., Hendy, C.H., 1984. 13C Record of benthic foraminifera in the last interglacial ocean: implications for the carbon cycle and the global deep water circulation. Quaternary Research 21, 225–243.

Duplessy, J.C., Shackleton, N.J., Fairbanks, R.G., Labeyrie, L., Oppo, D., Kallel, N., 1988. Deepwater source variations during the last climatic cycle and their impact on the global deepwater circulation. Paleoceanography 3, 343–360.

Elliot, M., Labeyrie, L., Bond, G.C., Cortijo, E., Turon, J.L., Tisnerat, N., Duplessy, J.C., 1998. Millennial-scale iceberg discharges in the Irminger Basin during the last glacial period: relationship with the Heinrich events and environmental settings. Paleoceanography 13, 433–446.

Fairbanks, R.G., Sverdlove, M., Free, R., Wiebe, P.H., Be, A.W.H., 1982. Vertical distribution and isotopic fractionation of living planktonic foraminifera from the Panama Basin. Nature 298, 841–844.

Flower, B.P., Oppo, D.W., McManus, J.F., Venz, K.A., Hodell, D.A., Cullen, J.L., 2000. North Atlantic intermediate to deep water circulation and chemical stratification during the past 1 Myr. Paleoceanography 15, 388–403.

Grousset, F.E., Labeyrie, L., Sinko, J.A., Cremer, M., Bond, G., Duprat, J., Cortijo, E., Huon, S., 1993. Patterns of ice-rafted detritus in the glacial North Atlantic (40–55°N). Paleoceanography 8, 175–192.

Grützner, J., Higgins, S.M., 2010. Threshold behavior of millennial scale variability in deep water hydrography inferred from a 1.1 Ma long record of sediment provenance at the southern Gardar Drift. Paleoceanography 25, PA4204. doi:10.1029/2009PA001873.

Hatun, H., Sando, A.B., Drange, H., Hansen, B., Valdimarsson, H., 2005. Influence of the Atlantic Subpolar Gyre on the thermohaline circulation. Science 309, 1841–1844.

Heinrich, H., 1988. Origin and consequences of cyclic ice rafting in the Northeast Atlantic Ocean during the past 130,000 years. Quaternary Research 29, 142–152.

Hemming, S.R., 2004. Heinrich events: massive late Pleistocene detritus layers of the North Atlantic and their global climate imprint. Reviews in Geophysics 42, RG1005. doi:10.1029/2003RG000128.

Hemming, S.R., Broecker, W.S., Sharp, W.D., Bond, G.C., Gwiazda, R.H., McManus, J.F., Klas, M., Hajdas, I., 1998. Provenance of Heinrich layers in core V28-82, northeastern Atlantic: $^{40}Ar/^{39}Ar$ ages of ice-rafted hornblende, Pb isotopes in feldspar grains, and Nd–Sr–Pb isotopes in the fine sediment fraction. Earth and Planetary Science Letters 164, 317–333.

Hodell, D.A., Venz-Curtis, K.A., 2006. Late Neogene history of deepwater ventilation in the Southern Ocean. Geochemistry Geophysics Geosystems 7, Q09001. 10.01029/02005GC001211.

Hodell, D.A., Venz, K.A., Charles, C.D., Ninnemann, U.S., 2003. Pleistocene vertical carbon isotope and carbonate gradients in the South Atlantic sector of the Southern Ocean. Geochemistry Geophysics Geosystems 4, 1004. doi:10.1029/2002GC000367.

Hodell, D.A., Channell, J.E.T., Curtis, J.H., Romero, O.E., Röhl, U., 2008. Onset of "Hudson Strait" Heinrich events in the eastern North Atlantic at the end of the middle Pleistocene transition (~640 ka)? Paleoceanography 23.

Hodell, D.A., Evans, H.F., Channell, J.E.T., Curtis, J.H., 2010. Phase relationships of North Atlantic ice-rafted debris and surface-deep climate proxies during the last glacial period. Quaternary Science Reviews 29, 3875–3886.

Imbrie, J., Berger, A., Boyle, E.A., Clemens, S.C., Duffy, A., Howard, W.R., Kukla, G., Kutzbach, J., Martinson, D.G., McIntyre, A., Mix, A.C., Molfino, B., Morley, J.J., Peterson, L.C., Pisias, N.G., Prell, W.L., Raymo, M.E., Shackleton, N.J., Toggweiler, J.R., 1993. On the structure and origin of major glaciation cycles 2. The 100,000-year cycle. Paleoceanography 8, 699–735.

Jansen, J.H.F., Kuijpers, A., Troelstra, S.R., 1986. A Mid-Brunhes climatic event: long-term changes in global atmosphere and ocean circulation. Science 232, 619–622.

Jonkers, L., Moros, M., Prins, M.A., Dokken, T., Dahl, C.A., Dijkstra, N., Perner, K., Brummer, G.-J.A., 2010. A reconstruction of sea surface warming in the northern North Atlantic during MIS 3 ice-rafting events. Quaternary Science Reviews 29, 1791–1800.

Jouzel, J., Masson-Delmotte, V., Cattani, O., Dreyfus, G., Falourd, S., Hoffmann, G., Minster, B., Nouet, J., Barnola, J.M., Chappellaz, J., Fischer, H., Gallet, J.C., Johnsen, S., Leuenberger, M., Loulergue, L., Luethi, D., Oerter, H., Parrenin, F., Raisbeck, G., Raynaud, D., Schilt, A., Schwander, J., Selmo, E., Souchez, R., Spahni, R., Stauffer, B., Steffensen, J.P., Stenni, B., Stocker, T.F., Tison, J.L., Werner, M., Wolff, E.W., 2007. Orbital and millennial antarctic climate variability over the past 800,000 years. Science 317, 793–796.

Kleiven, H.F., Jansen, E., Curry, W.B., Hodell, D.A., Venz, K.A., 2003. Atlantic Ocean thermohaline circulation changes on orbital to suborbital timescales during the mid-Pleistocene. Paleoceanography 18, 1008.

Kucera, M., Weinelt, M., Kiefer, T., Pflaumann, U., Hayes, A., Weinelt, M., Chen, M.-T., Mix, A.C., Barrows, T.T., Cortijo, E., Duprat, J., Juggins, S., Waelbroeck, C., 2005. Reconstruction of sea-surface temperatures from assemblages of planktonic foraminifera: multi-technique approach based on geographically constrained calibration data sets and its application to glacial Atlantic and Pacific Oceans. Quaternary Science Reviews 24, 951–998.

Lisiecki, L.E., Raymo, M.E., 2005. A Pliocene–Pleistocene stack of globally distributed benthic δ18O records. Paleoceanography 20. doi:10.1029/2004PA001071.

Locarnini, R.A., Mishonov, A.V., Antonov, J.I., Boyer, T.P., Garcia, H.E., 2006. Temperature. In: Levitus, S. (Ed.), World Ocean Atlas 2005, vol. 1. U.S. Government Printing Office, Washington, D.C.

Luthi, D., Le Floch, M., Bereiter, B., Blunier, T., Barnola, J.-M., Siegenthaler, U., Raynaud, D., Jouzel, J., Fischer, H., Kawamura, K., Stocker, T.F., 2008. High-resolution carbon dioxide concentration record 650,000–800,000 years before present. Nature 453, 379–382.

Malmgren, B.r.A., Kucera, M., Nyberg, J., Waelbroeck, C., 2001. Comparison of statistical and artificial neural network techniques for estimating past sea surface temperatures from planktonic foraminifer census data. Paleoceanography 16, 520–530.

Marchitto, T.M., Broecker, W.S., 2006. Deep water mass geometry in the glacial Atlantic Ocean: a review of constraints from the paleonutrient proxy Cd/Ca. Geochemistry Geophysics Geosystems 7, Q12003.

Marotzke, J., 1989. Instabilities and multiple steady states of the thermohaline circulation. In: Anderson, D.L.T., Willebrand, J. (Eds.), Ocean Circulation Models: Combining Data and Dynamics. NATO ASI Series, pp. 501–511.

Maslin, M.A., Ridgwell, A.J., 2005. Mid-Pleistocene revolution and the 'eccentricity myth'. In: Geological Society, London, Special Publications, vol. 247, 19–34 pp.

McCorkle, D.C., Keigwin, L.D., Corliss, B.H., Emerson, S.R., 1990. The influence of microhabitats on the carbon isotopic composition of deep-sea benthic foraminifera. Paleoceanography 5, 161–185. doi:10.1029/PA1005i1002p00161.

McManus, J.F., Oppo, D.W., Cullen, J.L., 1999. A 0.5-million-year record of millennial-scale climate variability in the North Atlantic. Science 283, 971–975.

McManus, J.F., Oppo, D.W., Keigwin, L.D., Cullen, J.L., Bond, G.C., 2002. Thermohaline Circulation and Prolonged Interglacial Warmth in the North Atlantic. Quaternary Research 58, 17–21.

Mignot, J., Ganopolski, A., Levermann, A., 2007. Atlantic subsurface temperatures: response to a shutdown of the overturning circulation and consequences for its recovery. Journal of Climate 20, 4884–4898.

Moros, M., Kuijpers, A., Snowball, I., Lassen, S., Bäckström, D., Gingele, F., McManus, J., 2002. Were glacial iceberg surges in the North Atlantic triggered by climatic warming? Marine Geology 192, 393–417.

Moros, M., McManus, J.F., Rasmussen, T., Kuijpers, A., Dokken, T., Snowball, I., Nielsen, T., Jansen, E., 2004. Quartz content and the quartz-to-plagioclase ratio determined by X-ray diffraction: a proxy for ice rafting in the northern North Atlantic? Earth and Planetary Science Letters 218, 389–401.

Mudelsee, M., Schulz, M., 1997. The Mid-Pleistocene climate transition: onset of 100 ka cycle lags ice volume build-up by 280 ka. Earth and Planetary Science Letters 151, 117–123.

Mudelsee, M., Stattegger, K., 1997. Exploring the structure of the mid-Pleistocene revolution with advanced methods of time-series analysis. Geologische Rundschau 86, 499–511.

Nyland, B.F., Jansen, E., Elderfield, H., Andersson, C., 2006. Neogloboquadrina pachyderma (dex. and sin.) Mg/Ca and d18O records from the Norwegian Sea. Geochemistry Geophysics Geosystems 7, Q10P17. doi:10.1029/2005GC001055.

Oppo, D.W., Fairbanks, R.G., 1987. Variability in the deep and intermediate water circulation of the Atlantic Ocean during the past 25,000 years: Northern Hemisphere modulation of the Southern Ocean. Earth and Planetary Science Letters 86, 1–15.

Oppo, D.W., Lehman, S.J., 1993. Mid-depth circulation of the subpolar north atlantic during the last glacial maximum. Science 259, 1148–1152.

Oppo, D.W., Raymo, M.E., Lohmann, G.P., Mix, A.C., Wright, J.D., Prell, W.L., 1995. A d13C record of upper North Atlantic deep water during the past 2.6 million years. Paleoceanography 10, 373–394.

Oppo, D.W., McManus, J.F., Cullen, J.L., 1998. Abrupt climate events 500,000 to 340,000 years ago: evidence from subpolar North Atlantic Sediments. Science 279, 1335–1338.

Oppo, D.W., Keigwin, L.D., McManus, J.F., Cullen, J.L., 2001. Persistent suborbital climate variability in marine isotope stage 5 and termination II. Paleoceanography 16, 280–292.

Oppo, D.W., McManus, J.F., Cullen, J.L., 2006. Evolution and demise of the Last Interglacial warmth in the subpolar North Atlantic. Quaternary Science Reviews 25, 3268–3277.

Paillard, D., Labeyrie, L., Yiou, P., 1996. Macintosh program performs time-series analysis. EOS 77, 379.

Parrenin, F., Barnola, J.M., Beer, J., Blunier, T., Castellano, E., Chappellaz, J., Dreyfus, G., Fischer, H., Fujita, S., Jouzel, J., Kawamura, K., Lemieux-Dudon, B., Loulergue, L., Masson-Delmotte, V., Narcisi, B., Petit, J.R., Raisbeck, G., Raynaud, D., Ruth, U., Schwander, J., Severi, M., Spahni, R., Steffensen, J.P., Svensson, A., Udisti, R., Waelbroeck, C., Wolff, E., 2007. The EDC3 chronology for the EPICA Dome C ice core. Climates Past 3, 485–497.

Paul, A., Schulz, M., 2002. Holocene climate variability on centennial- to-millennial time scales: 2. Internal and forced oscillations as possible cause. In: Wefer, G., Berger, W., Behre, K.-E., Jansen, E. (Eds.), Climate Development and History of the North Atlantic Realm. s. Springer-Verlag, Berlin Heidelberg, pp. 77–88.

Peck, V.L., Hall, I.R., Zahn, R., Elderfield, H., 2008. Millennial-scale surface and subsurface paleothermometry from the northeast Atlantic, 55–8 ka BP. Paleoceanography 23.

Prell, W.L., 1985. The stability of low-latitude sea-surface temperatures: an evaluation of the CLIMAP reconstruction with emphasis on the positive SST anomalies, Washington, D.C.

Rasmussen, T.L., Thomsen, E., 2004. The role of the North Atlantic Drift in the millennial timescale glacial climate fluctuations. Palaeogeography, Palaeoclimatology, Palaeoecology 210, 101–116.

Raymo, M.E., Ruddiman, W.F., Shackleton, N.J., Oppo, D.W., 1990. Evolution of Atlantic-Pacific d13C gradients over the last 2.5 m.y. Earth and Planetary Science Letters 97, 353–368.

Raymo, M.E., Oppo, D.W., Curry, W.B., 1997. The mid-Pleistocene climate transition: A deep sea carbon isotopic perspective. Paleoceanography 12, 546–559.

Raymo, M.E., Ganley, K., Carter, S., Oppo, D.W., McManus, J., 1998. Millennial-scale climate instability during the early Pleistocene epoch. Nature 392, 699–702.

Raymo, M.E., Oppo, D.W., Flower, B.P., Hodell, D.A., McManus, J.F., Venz, K.A., Kleiven, H.F., McIntyre, K., 2004. Stability of North Atlantic water masses in face of pronounced climate variability during the Pleistocene. Paleoceanography 19. doi:10.1029/2003PA000921.

Reynolds-Sautter, L., Thunell, R.C., 1989. Seasonal succession of planktonic foraminifera; results from a four-year time-series sediment trap experiment in the Northeast Pacific. Journal of Foraminiferal Research 19, 253–267.

Reynolds-Sautter, L., Thunell, R.C., 1991. Seasonal variability in the d18O andd13C of planktonic foraminifera from an upwelling environment: sediment trap results from the San Pedro Basin, Southern California Bight. Paleoceanography 6, 307–334.

Risebrobakken, B., Dokken, T., Otterå, O.H., Jansen, E., Gao, Y., Drange, H., 2007. Inception of the Northern European ice sheet due to contrasting ocean and insolation forcing. Quaternary Research 67, 128–135.

Rohling, E.J., Marsh, R., Wells, N.C., Siddall, M., Edwards, N.R., 2004. Similar melt-water contributions to glacial sea level changes from Antarctic and northern ice sheets. Nature 430, 1016–1021.

Rohling, E.J., Grant, K., Hemleben, C., Kucera, M., Roberts, A.P., Schmeltzer, I., Schulz, H., Siccha, M., Siddall, M., Trommer, G., 2008. New constraints on the timing of sea level fluctuations during early to middle marine isotope stage 3. Paleoceanography 23, PA3219.

Ruddiman, W.F., 1977. Late Quaternary deposition of ice rafted sand in the subpolar North Atlantic (lat 40° to 65° N). Geological Society of America Bulletin 88, 1813–1827.

Ruddiman, W.F., McIntyre, A., 1979. Warmth of the subpolar North Atlantic Ocean during northern hemisphere ice-sheet growth. Science 204, 173–175.

Ruddiman, W.F., McIntyre, A., 1981. Oceanic mechanisms for amplification of the 23,000-year ice-volume cycle. Science 212, 617–627.

Ruddiman, W.F., McIntyre, A., Niebler-Hunt, V., Durazzi, J.T., 1980. Oceanic evidence for the mechanism of rapid northern hemisphere glaciation. Quaternary Research 13, 33–64.

Schiebel, R., Hemleben, C., 2000. Interannual variability of planktic foraminiferal populations and test flux in the eastern North Atlantic Ocean (JGOFS). Deep Sea Research Part II: Topical Studies in Oceanography 47, 1809–1852.

Schiebel, R., Waniek, J., Bork, M., Hemleben, C., 2001. Planktic foraminiferal production stimulated by chlorophyll redistribution and entrainment of nutrients. Deep Sea Research Part I: Oceanographic Research Papers 48, 721–740.

Schmitz, W.J., McCartney, M., 1993. On the North Atlantic circulation. Reviews in Geophysics 31, 29–49.

Shackleton, N.J., 1987. Oxygen isotopes, ice volume and sea level. Quaternary Science Reviews 6, 183–190.

Shackleton, N.J., Hall, M.A., 1984. Oxygen and carbon isotope stratigraphy of the deep sea drilling project hole 552A: Plio-Pleistocene glacial history. Initial Reports DSDP 81, 599–609.

Shackleton, N.J., Hall, M.A., Vincent, E., 2000. Phase relationships between millennial-scale events 64,000-24,000 years ago. Paleoceanography 15, 565–569.

Siddall, M., Rohling, E.J., Almogi-Labin, A., Hemleben, C., Meischner, D., Schmelzer, I., Smeed, D.A., 2003. Sea-level fluctuations during the last glacial cycle. Nature 423, 853–858.

Siddall, M., Stocker, T.F., Blunier, T., Spahni, R., McManus, J.F., Bard, E., 2006. Using a maximum simplicity paleoclimate model to simulate millennial variability during the last four glacial periods. Quaternary Science Reviews 25, 3185–3197.

Siddall, M., Rohling, E.J., Thompson, W.G., Waelbroeck, C., 2008. Marine isotope stage 3 sea level fluctuations: data synthesis and new outlook. Reviews in Geophysics 46, RG4003. doi:10.1029/2007RG000226.

Siegenthaler, U., Stocker, T.F., Monnin, E., Luthi, D., Schwander, J., Stauffer, B., Raynaud, D., Barnola, J.-M., Fischer, H., Masson-Delmotte, V., Jouzel, J., 2005. Stable carbon cycle–climate relationship during the Late Pleistocene. Science 310, 1313–1317.

Sierro, F.J., Andersen, N., Bassetti, M.A., Berné, S., Canals, M., Curtis, J.H., Dennielou, B., Flores, J.A., Frigola, J., Gonzalez-Mora, B., Grimalt, J.O., Hodell, D.A., Jouet, G., Pérez-Folgado, M., Schneider, R., 2009. Phase relationship between sea level and abrupt climate change. Quaternary Science Reviews 28, 2867–2881.

Skinner, L.C., Elderfield, H., 2007. Rapid fluctuations in the deep North Atlantic heat budget during the last glacial period. Paleoceanography 22, PA1205. doi:10.1029/2006PA001338.

Skinner, L.C., Shackleton, N.J., Elderfield, H., 2003. Millennial-scale variability of deep-water temperature and d18Odw indicating deep-water source variations in the Northeast Atlantic, 0–34 cal. ka BP. Geochemistry Geophysics Geosystems 4, 1098. doi:10.1029/2003GC000585.

Stein, R., Hefter, J., Grützner, J., Voelker, A., Naafs, B.D.A., 2009. Variability of surface water characteristics and Heinrich-like events in the Pleistocene midlatitude North Atlantic Ocean: biomarker and XRD records from IODP Site U1313 (MIS 16–9). Paleoceanography 24.

Suganuma, Y., Yokoyama, Y., Yamazaki, T., Kawamura, K., Horng, C.-S., Matsuzaki, H., 2010. 10Be evidence for delayed acquisition of remanent magnetization in marine sediments: implication for a new age for the Matuyama-Brunhes boundary. Earth and Planetary Science Letters 296, 443–450.

Tzedakis, P.C., Raynaud, D., McManus, J.F., Berger, A., Brovkin, V., Kiefer, T., 2009. Interglacial diversity. Nature Geoscience 2, 751–755.

Van Aken, H.M., De Boer, C.J., 1995. On the synoptic hydrography of intermediate and deep water masses in the Iceland Basin. Deep Sea Research Part I: Oceanographic Research Papers 42, 165–189.

van Kreveld, S., Sarnthein, M., Erlenkeuser, H., Grootes, P., Jung, S., Nadeau, M.J., Pflaumann, U., Voelker, A., 2000. Potential links between surging ice sheets, circulation changes, and the Dansgaard-Oeschger cycles in the Irminger Sea, 60–18 kyr. Paleoceanography 15, 425–442. doi:10.1029/1999PA000464.

Venz, K.A., Hodell, D.A., 2002. New evidence for changes in Plio-Pleistocene deep water circulation from Southern Ocean ODP Leg 177 Site 1090. Palaeogeography, Palaeoclimatology, Palaeoecology 182, 197–220.

Venz, K.A., Hodell, D.A., Stanton, C., Warnke, D.A., 1999. A 1.0 Myr record of Glacial North Atlantic intermediate water variability from ODP site 982 in the northeast Atlantic. Paleoceanography 14, 42–52.

Weaver, A.J., 1999. Millennial timescale variability in ocean/climate models. In: Clark, P.U., Webb, R.S., Keigwin, L.D. (Eds.), Mechanisms of Global Climate Change at Millennial Time Scales. AGU, Washington, DC, pp. 285–300.

Winton, M., 1997. The effect of cold climate upon north atlantic deep water formation in a simple ocean–atmosphere model. Journal of Climate 10, 37–51.

Wright, A.K., Flower, B.P., 2002. Surface and deep ocean circulation in the subpolar North Atlantic during the mid-Pleistocene revolution. Paleoceanography 17, 1068.

Wright, D.G., Stocker, T.F., 1991. A zonally averaged ocean model for the thermohaline circulation. Part I: model development and flow dynamics. Journal of Physical Oceanography 21, 1713–1724.

Yu, J., Elderfield, H., Piotrowski, A.M., 2008. Seawater carbonate ion-[delta]13C systematics and application to glacial-interglacial North Atlantic ocean circulation. Earth and Planetary Science Letters 271, 209–220.